

Kinematic of a Mobile Manipulator of 8 Degrees of Freedom for Inspection Tasks

C. Angie J. Valencia, Oscar F. Aviles and Mauricio F. Mauledoux
Department of Mechatronics Engineering, Faculty of Engineering,
Militar Nueva Granada University, Bogota, Colombia

Abstract: A mobile manipulator is made up of an arm, a wrist and a tool of clasp, designed to move inside a workspace that increases with the Degrees of Freedom (DOF) of the system, defined as the number of longitudinal or rotational displacements in the mechanism. These arms are implemented in inspection tasks in which they are provisions on mobile platforms that determine their movement from the contribution that each wheel provide for the locomotion in function of the system restrictions (limitation to roll laterally or rotate on its own axis). To understand the operation of these mechanisms, the first thing to do is to describe the kinematic model of the platform considering the calculation of the direct kinematic of five DOF manipulator as well as the calculation of the inverse kinematic to obtain the ideal trajectory for the movement from one point to another through Newton-Raphson algorithms implementation. Besides, stipulating the expressions of global movement of the vehicle in terms of the individual geometry of the wheels that make up the mechanism, modeled as a rigid body with wheels that is handled on the horizontal plane in three different axes, two of position in the plane and one of the orientation along the vertical axis.

Key words: Degrees of freedom, direct kinematic, generalized coordinates, inverse kinematic, manipulator robot, mobile robot, Newton-Raphson

INTRODUCTION

A manipulator arm is defined as a set of rigid elements connected in series using prismatic or revolution joints with a relative movement of different elements, resulting in the displacement of the final tool or end effector (Apostolovich, 2009). In this, the start of the chain or first link must be attached or fixed to a support base while the other end may be attached or free (closed kinematic chain or open kinematic chain, respectively) and sometimes equipped with tools for the manipulation of objects or specific tasks (Romero, 2012).

The manipulators are made up of elements such as: mechanical structure, actuators, sensors, controllers and manipulator elements. As for the mechanical structure, the robot is formed by a series of elements or links that are joined by 6 type of joints that allow them to have a relative movement between them: spherical joint which combines three turns in 3 directions:

- Planar which allows movement on a plane
- Prismatic which allows translation along an axis
- Rotational, allowing rotation around a single axis and cylindrical which brings together a rotation a translation movement (Baturone, 2001)

On the other hand, a mobile robot needs locomotion mechanisms for its displacement through structured and unstructured environments. Currently, there is a wide variety of possible motion systems, so, selecting the appropriate depend of the application is an important aspect in the design of mobile robots.

For the study of the behaviors of the mobile platform, we have the kinematic model considered as the basic study to understand the movement of mechanical systems. In mobile robot, it is necessary to understand this behavior, to design mechanisms for inspection tasks, in addition to the possibility of creating controllers that allow to improve its operation (Craig, 1989). Within the variables to be considered for the management of the mobile platform, is the workspace that is defined as the range of possibilities that the platform can reach in each environment, in addition to its controllability in which the possible trajectories in said space.

For the study of the behavior of a manipulator we define the kinematics that relates the space of the articular trajectories $q_1, q_2, q_3, \dots, q_n$ with the Cartesian space disposed at the end of it. In addition, it is defined as the basis of the dynamic studies for the calculation of the forces that are required to cause movement in the system (Ninu, 2013; Saquimux, 2005).

MATERIALS AND METHODS

Mobile manipulator robot kinematics: For the development of the present work we consider the scheme of Fig. 1 where the structure of the mobile manipulator is specified. It should be that for the kinematic calculations of the mechanism, a kinematic decoupling is contemplated, between the mobile platform and the manipulator whereby the frame of reference and movement of the manipulator is considered at the beginning of the kinematic chain but not as the set of global coordinates of the hybrid platform. For notation:

$$\begin{aligned} s_1 &= \sin(\theta_1), c_1 = \cos(\theta_1), \\ c_{(\beta_1)} &= \cos(\beta_1), s_{(\beta_1)} = \sin(\beta_1), \\ c_{(\alpha_1+\beta_1)} &= \cos(\beta_1), c_{(\alpha_1+\beta_1)} = \sin(\alpha_1+\beta_1) \end{aligned}$$

Manipulator kinematics: When performing the kinematic uncoupling in Fig. 2, the configuration diagram of the manipulator is presented where the articulations and coordinate axes describing their movement are specified.

Direct kinematic: The direct kinematics is that given the position and orientation of the final element of a manipulator, the values of the parameters of the joints can be determined. For this, the Denavit-Hartenberg (Hernandez, 2014), formulation is used which allows to obtain the homogeneous matrices based on the characteristics of the manipulator specified in Table 1.

Then, the matrices that allow to relate the coordinate systems based on the movements that the first system must make to reach the same position and orientation as its next system are developed. From the above in Eq. 1 is shown the system 0-1 matrix transformation, in Eq. 2, the 1-2 system matrix transformation, in Eq. 3, the 2-3 system matrix transformation, in Eq. 4, the 3-4 system matrix transformation and finally, in Eq. 5, the 4-5 system matrix transformation:

$$T_{01} = \begin{bmatrix} c_1 & 0 & s_1 & 0 \\ s_1 & 0 & -c_1 & 0 \\ 0 & 1 & 0 & l_1 \\ 0 & 0 & 0 & 1 \end{bmatrix} \quad (1)$$

$$T_{12} = \begin{bmatrix} c_2 & -s_2 & 0 & l_2 \times c_2 \\ s_2 & c_2 & 0 & l_2 \times s_2 \\ 0 & 0 & 1 & 0 \\ 0 & 0 & 0 & 1 \end{bmatrix} \quad (2)$$

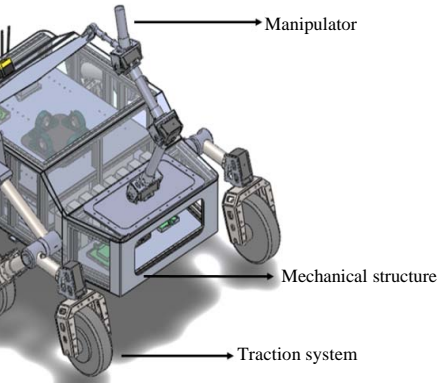


Fig. 1: Hybrid platform scheme

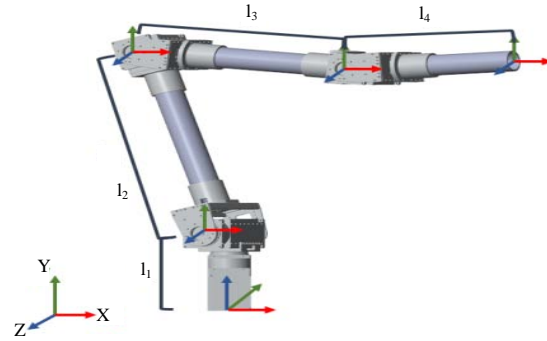


Fig. 2: Five DOF arm scheme

Table 1: Denavit-hartenberg matrix

Articulations	θ_i	d_i	a_i	c_i
1	θ_1	l_1	0	90
2	θ_2	0	l_2	0
3	θ_3	0	l_3	0
4	θ_4	0	l_4	-90
5	θ_5	l_5	0	0

$$T_{23} = \begin{bmatrix} c_3 & -s_3 & 0 & l_3 \times c_3 \\ s_3 & c_3 & 0 & l_3 \times s_3 \\ 0 & 0 & 1 & 0 \\ 0 & 0 & 0 & 1 \end{bmatrix} \quad (3)$$

$$T_{23} = \begin{bmatrix} 0 & -s_4 & c_4 & l_4 \times c_4 \\ 0 & c_4 & s_4 & l_4 \times s_4 \\ -1 & 0 & 0 & 0 \\ 0 & 0 & 0 & 1 \end{bmatrix} \quad (4)$$

$$T_{45} = \begin{bmatrix} c_5 & -s_5 & 0 & 0 \\ s_5 & c_5 & 0 & 0 \\ 0 & 0 & 1 & l_5 \\ 0 & 0 & 0 & 1 \end{bmatrix} \quad (5)$$

Once, the transformation matrices of each system have been defined, the multiplication of these matrices is done to obtain the transformation matrix T_{05} which describes the kinematics of the coordinate system of the final effector with respect to the coordinate reference system as observed in Eq. 6:

$$T_{05} = \begin{bmatrix} R_{3 \times 3} & P_{3 \times 3} \\ F_{1 \times 3} & W_{1 \times 1} \end{bmatrix} = \begin{bmatrix} Rot & Tras \\ P_{ersp} & F_{escala} \end{bmatrix} \quad (6)$$

From the total transformation matrix, the translation vector P is extracted because in this the position of the final link of the manipulator in the coordinate axes X, Y and Z, respectively is found which will be used in the optimization algorithm developed for the calculation of the robot's inverse kinematics.

Inverse kinematic: The problem of inverse kinematics is that given a position and orientation of the end effector the values of the angles in the joints that make up the manipulator system must be determined, becoming a complicated problem because there are multiple solutions for the same position and orientation of the final element (Loukianov *et al.*, 1997; Takahashi and Kawamura, 2000).

In order to solve the problem of inverse kinematics, the system will be considered an optimization problem that will be solved by Newton-Raphson's method of successive approximations, due to in the algorithm the iteration error does not define the behavior of the following, so there is no accumulation error that generates unwanted trajectories or infinite speeds in the joints (Qu and Xu, 2011; Benhabib *et al.*, 1985; Goldenberg *et al.*, 1985). From the above, in Eq. 7 the cost function to be optimized by the algorithm is defined:

$$\begin{bmatrix} \theta_1(i+1) \\ \theta_2(i+1) \\ \theta_3(i+1) \\ \theta_4(i+1) \end{bmatrix} = \begin{bmatrix} \theta_1 \\ \theta_2 \\ \theta_3 \\ \theta_4 \end{bmatrix} - \frac{f(\theta_1(i), \theta_2(i), \theta_3(i), \theta_4(i))}{f'(\theta_1(i), \theta_2(i), \theta_3(i), \theta_4(i))} \quad (7)$$

Where, the cost function $f(x)$, is defined as the position vector in X, Y and Z of the final link, obtained from the direct kinematic as is shown in Eq. 8 and determinate multiplying the transformation matrices and expressed for X in Eq. 9 for Y in Eq. 10 and Z in Eq. 11:

$$f(\theta_1, \theta_2, \theta_3, \theta_4) = \begin{bmatrix} X_d - X \\ Y_d - Y \\ Z_d - Z \end{bmatrix} \quad (8)$$

$$X = l_2 \times c_1 \times c_2 - l_3 \times s_4 \times (c_3 \times c_1 \times s_2 + s_3 \times c_1 \times c_2) + l_3 \times c_4 \times (c_3 \times c_1 \times c_2 - s_3 \times c_1 \times s_2) + l_3 \times c_3 \times c_1 \times c_2 - l_3 \times s_3 \times c_1 \times s_2 \quad (9)$$

$$Y = l_3 \times c_4 \times (c_3 \times c_2 \times s_1 - s_3 \times s_1 \times s_2) + l_3 \times c_3 \times c_2 \times s_1 + l_2 \times c_2 \times s_1 - l_3 \times s_4 \times (s_3 \times c_2 \times s_1 + c_3 \times s_1 \times s_2) - l_3 \times s_3 \times s_1 \times s_2 \quad (10)$$

$$Z = l_1 + l_2 \times s_2 + l_3 \times c_4 \times (c_2 \times s_3 + c_3 \times s_2) + l_3 \times c_2 \times s_3 + l_3 \times c_3 \times s_2 + l_3 \times s_4 \times (c_2 \times c_3 - s_2 \times s_3) \quad (11)$$

The algorithm ends when the difference between desired position and the current has a value a minor to 1×10^{-6} as is shown in Eq. 12:

$$e = \sqrt{(X_d - X)^2 + (Y_d - Y)^2 + (Z_d - Z)^2} \leq 1 \times 10^{-6} \quad (12)$$

Next, we describe the pseudo-code to develop it for the calculation of the posture of the robot manipulator of 5 degrees of freedom (Algorithm 1).

Algorithm 1; Newton Raphson algorithm:

```

Begin
   $x_1$  - initial point
   $\epsilon$  - tolerance
  k-1
  Calculate  $f'(x_1)$ 
  While  $f'(x_{k+1}) \geq \epsilon$ 
     $x_{k+1} = x_k - f(x_k)/f'(x_k)$ 
    K=k+1
    Calculate  $f'(x_k)$ 
  End while
  Plot x

```

Mobile platform kinematics: For the calculation of the kinematics of the mobile platform, the configuration scheme for obtaining the kinematic model of the robot is defined in which the restrictions of movement of the independent wheels are expressed, through the physical decomposition of the robotic platform with the purpose of defining the wheels and their configurations. Therefore, Fig. 3 shows the configuration to be managed and Table 2 defines the variables that characterize it.

Where γ_i represents the value of rotation of each of the wheels determined by the calculation of the instantaneous center of rotation.

Figure 3 is observed that the platform consists of 6 wheels which two are fixed and the other 4 are steerable. From there, in Fig. 4 is shown the wheel's configuration with its respectively mathematical representation with Eq. 13 and 14:

$$[s(\alpha + \beta) - c(\alpha + \beta) - l \times c(\beta)] \times R(\theta) \times \xi_i - r\dot{\phi} = 0 \quad (13)$$

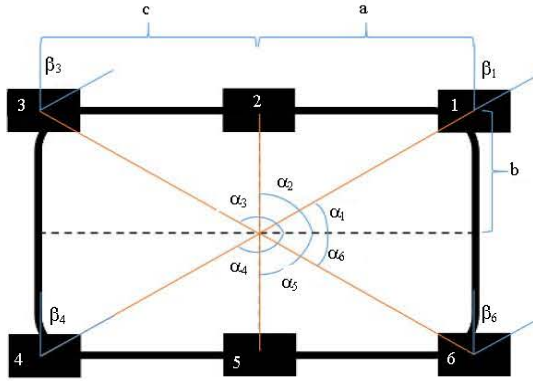


Fig. 3: Six wheels of robotic platform

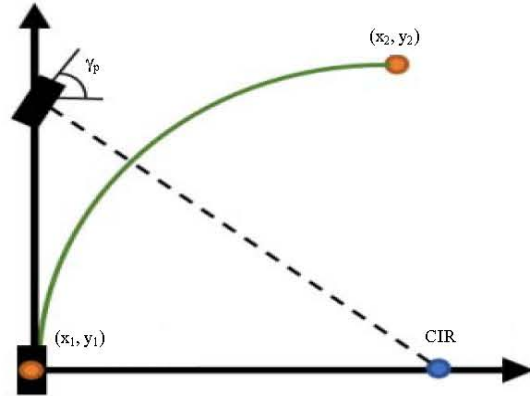


Fig. 5: Instantaneous Center of Rotation (CIR)

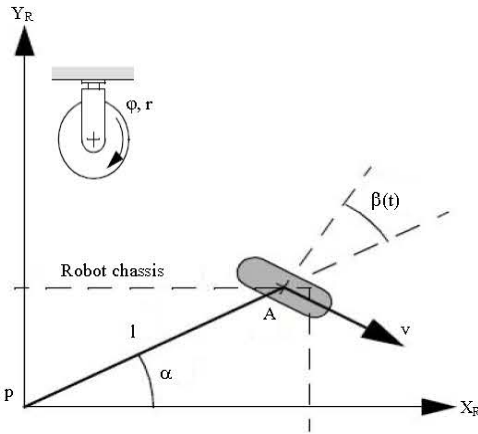


Fig. 4: Kinematic configurations of wheels

Table 2: Matrix of angular specifications

Angles	Values
α_1	$\tan^{-1}(b/2a)$
α_2	$\pi/2$
α_3	$\pi - \tan^{-1}(b/2c)$
α_4	$-\pi + \tan^{-1}(b/2c)$
α_5	$-\pi/2$
α_6	$-\tan^{-1}(b/2a)$
β_1	$(\pi/2 + \gamma_1) - \alpha_1$
β_2	0
β_3	$(\pi/2 + \gamma_3) - \alpha_2$
β_4	$(\pi/2 + \gamma_4) - 2\pi$
β_5	π
β_6	$(\pi/2 + \gamma_6) - \alpha_6$

$$[c(\alpha+\beta)s(\alpha+\beta)l \times s(\beta)] \times R(\theta) \times \xi_I - r\dot{\phi} = 0 \quad (14)$$

Where:

ξ_I = The global coordinates of the robot $[\dot{x}, \dot{y}, \dot{\theta}]^T$

r = An identity matrix composed of the radius of the wheels

$R(\theta)$ = The rotational transformation matrix that describes the robot orientations in a global coordinated plane as is shown in Eq. 15:

$$R(\theta) = \begin{bmatrix} c(\theta) & s(\theta) & 0 \\ -s(\theta) & c(\theta) & 0 \\ 0 & 0 & 1 \end{bmatrix} \quad (15)$$

We must consider, the models presented in Eq. 13 and 14 assume that in all the cases there is only one point of contact between the wheel and the surface and additionally there is no slip in the point (Mason, 2001).

Having the characteristic equations of the wheels, we proceed with the construction of the final kinematic representation describing the movement of the mobile robotic platform as shown in Eq. 16:

$$\xi_I = R(\theta)^{-1} \begin{bmatrix} s(\alpha_1 + \beta_1) - c(\alpha_1 + \beta_1) - l_1 \times c(\beta_1) \\ s(\alpha_2 + \beta_2) - c(\alpha_2 + \beta_2) - l_2 \times c(\beta_2) \\ s(\alpha_3 + \beta_3) - c(\alpha_3 + \beta_3) - l_3 \times c(\beta_3) \\ s(\alpha_4 + \beta_4) - c(\alpha_4 + \beta_4) - l_4 \times c(\beta_4) \\ s(\alpha_5 + \beta_5) - c(\alpha_5 + \beta_5) - l_5 \times c(\beta_5) \\ s(\alpha_6 + \beta_6) - c(\alpha_6 + \beta_6) - l_6 \times c(\beta_6) \end{bmatrix}^{-1} \times \begin{bmatrix} r_1 & 0 & 0 & 0 & 0 & 0 \\ 0 & r_2 & 0 & 0 & 0 & 0 \\ 0 & 0 & r_3 & 0 & 0 & 0 \\ 0 & 0 & 0 & r_4 & 0 & 0 \\ 0 & 0 & 0 & 0 & r_5 & 0 \\ 0 & 0 & 0 & 0 & 0 & r_6 \end{bmatrix} \times \begin{bmatrix} \dot{\phi}_1 \\ \dot{\phi}_2 \\ \dot{\phi}_3 \\ \dot{\phi}_4 \\ \dot{\phi}_5 \\ \dot{\phi}_6 \end{bmatrix} \quad (16)$$

Where:

l_i = The distance from the center of mass of the mobile platform and each wheel

ϕ_i = The velocity of each wheel

Calculation of instantaneous center of rotation: To calculate the instantaneous center of rotation the geometry raised in Fig. 5 is considered. So, we need the

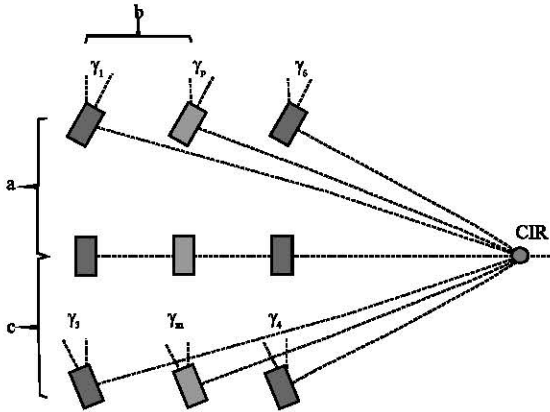


Fig. 6: Angular calculation of steerable wheels

Table 3: Angle of steerable wheels

Angles	Values
γ_1	$\cot^{-1}(\cot(\gamma_p)+b/2a)$
γ_3	$\cot^{-1}(\cot(\gamma_m)+b/2c)$
γ_4	$\cot^{-1}(\cot(\gamma_m)-b/2a)$
γ_6	$\cot^{-1}(\cot(\gamma_p)+b/2c)$

circumference equation to calculate the turn radius to be considered in the platform to move from (x_1, y_1) point to another in (x_2, y_2) .

To determinate the instantaneous center of rotation, we considered that (x_1, y_1) and (x_2, y_2) are circumference point with center in $c(h, k)$ and is located on the line $(r \times \cos(\theta) + x_1 \times r \times \sin(\theta) + y_1)$ with slope $m = \sin(\theta)/\cos(\theta)$. With the above, the characteristic equations of the circle are presented in Eq. 17 and since, we have 3 Eq. and 3 unknowns we proceed to solve the system of equations to obtain the values of h, k, r :

$$\begin{aligned} (x_1-h)^2 + (y_1-k)^2 &= r^2 \\ (x_2-h)^2 + (y_2-k)^2 &= r^2 \\ k-y_1-m(h-x_1) &= 0 \end{aligned} \quad (17)$$

The γ_p angle is calculated by geometry as is shown in Fig. 6 and Eq. 18 to calculate the γ_i angles described in Table 3:

$$\begin{aligned} \gamma_p &= \tan^{-1}\left(\frac{a}{|h-x_1|}\right) \\ \gamma_m &= \tan^{-1}\left(\frac{c}{|h-x_1|}\right) \end{aligned} \quad (18)$$

RESULTS AND DISCUSSION

Manipulator results: The kinematic manipulator algorithm is tested with an initial point of $[-20; -15; 20]$ and final

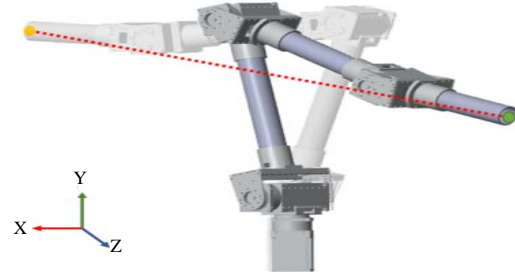


Fig. 7: Path of the front XY view manipulator

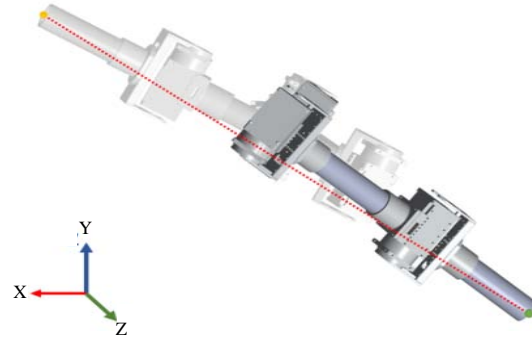


Fig. 8: Path of the front XZ view manipulator

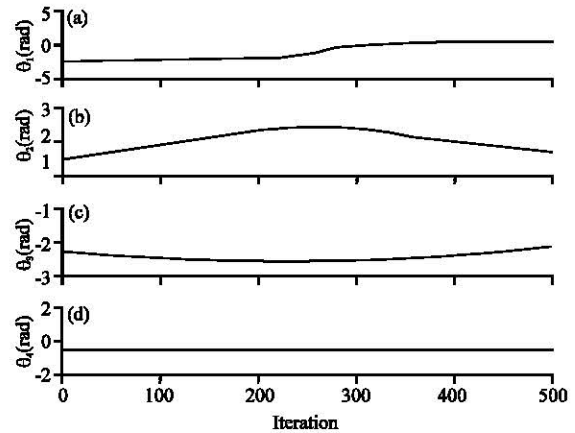


Fig. 9: Angular variation of the joints: a) Iteration 1; b) Iteration 2; c) Iteration 3 and d) Iteration 4

point of $[20; 10; 30]$ and a tolerance of 1×10^{-6} . So, we obtain Fig. 7 and 8 where is show the trajectory to be reached by the manipulator to get a desired final position and the Fig. 9, in which the variation realized by the angles of the articulations along the trajectory is shown.

The points chosen in the manipulator for the generation of the path ensure that the arm must pass through its center. The results of applying optimization algorithms show that to pass through this critical point

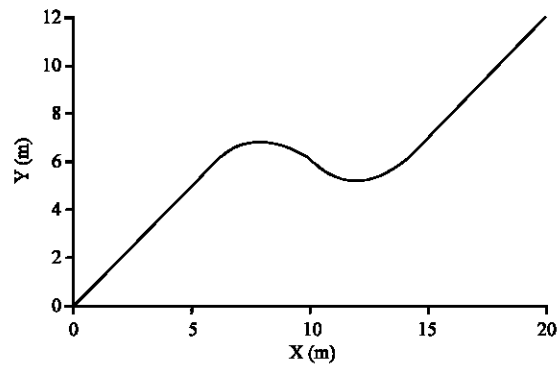


Fig. 10: Trajectory for the verification of the kinematics

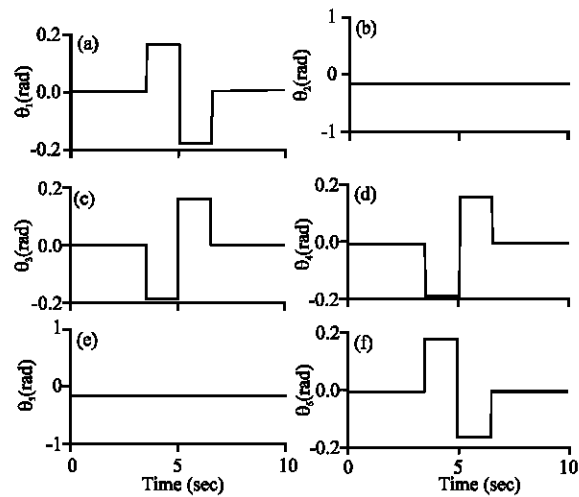


Fig. 11: Angles of the wheels that makes up the mechanism: a) Wheel 1; b) Wheel 2; c) Wheel 3; d) Wheel 4; e) Wheel 5 and f) Wheel 6

the manipulator follows a continuous path due to the iterative calculation of the angles calculated by the Newton-Raphson method which ensures that at no time will there exist singular positions or infinite speeds in the stipulated trajectories.

Mobile platform results: Angular variation of the joints to verify the correct calculation of the kinematics by wheels of the mobile robot is pre-established in Fig. 10, from which the angles are obtained for each wheel as shown in Fig. 11. Form the result obtained in Fig. 10 and 11, we proceed to make the calculus verification of the mobile platform kinematics, so we established an initial constant velocity ω of 10 rpm, from which the results of Fig. 12 were obtained.

Then tests are performed stipulating position, velocity and acceleration profiles in Fig. 13 that allows has a constant acceleration behavior in an interval of time due

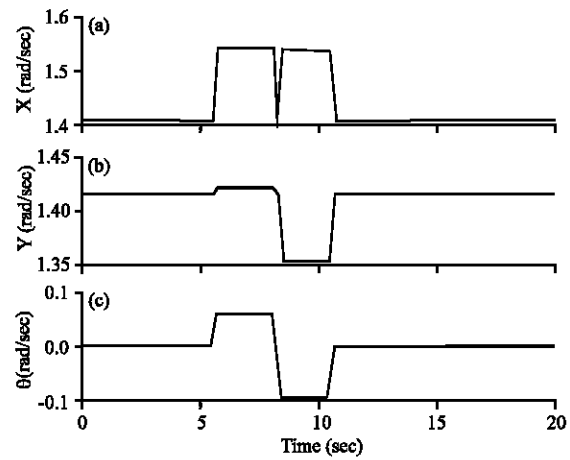


Fig. 12: Velocity in X, Y and θ of the mobile platform with constant velocity; a) X; b) Y and c) θ

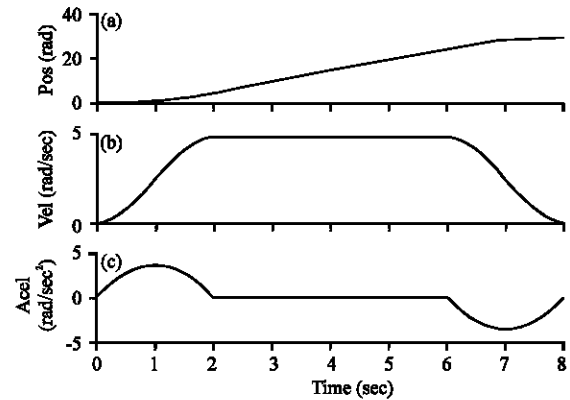


Fig. 13: Position, velocity and acceleration profile in platform movement: a) Acceleration; b) Velocity and c) Position

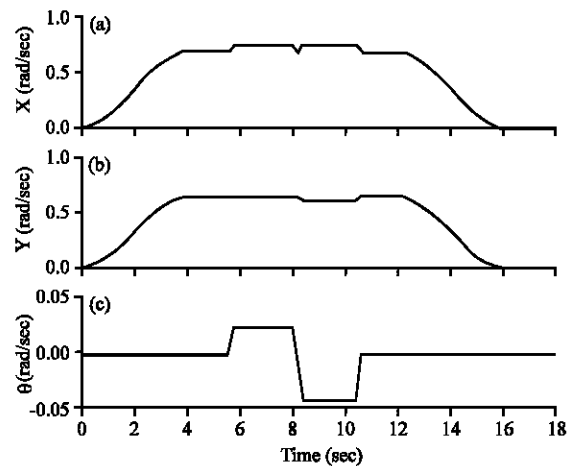


Fig. 14: Velocity in X, Y and θ of the mobile platform with the velocity profile: a) X; b) Y and c) θ

to it begins from an initial zero position and zero speed, then it has a constant velocity behavior and a zero acceleration value that ends with a deceleration process to end the trajectory with zero speed. From the above, we obtain the behaviors of Fig. 14, in X, Y and θ velocity.

CONCLUSION

By applying optimization techniques in the calculation of the inverse kinematics of a mobile manipulator, iterative angular configurations are obtained that permanently eliminate the infinite velocities produced by strong changes in angular variations, for example, from 0-180° in a sample of time. While for direct kinematics the only consideration to be considered is to correctly define the coordinate axes and degrees of freedom of the system because in some cases the final link where the gripper is located since, this link is assumed to be manipulated manually.

On the other hand, for the kinematics of the mobile platform it was observed that when performing tests with constant velocity and with velocity profiles the kinematics yields the velocities in X, Y and Z corresponding to the trajectory pre-established. So that, the correct calculation of the kinematic wheel difference specified in the previous sections is checked. This can be used for the subsequent calculation of the dynamics of the system since, it is based on the speed behavior of the 3 axes of movement of the platform (Campion *et al.*, 1996).

ACKNOWLEDGEMENT

The research for this study was supported by Nueva Granada Military University, through the project ING-IMP-2138

REFERENCES

- Apostolovich, L.F., 2009. [Modeling and dynamic simulation of a robotic arm of 4 degrees of freedom for tasks on a horizontal plane]. MSc Thesis, Pontifical Catholic University of Peru, Lima, Peru. (In Spanish)
- Baturone, A.O., 2001. [Robotica: Manipulators and Mobile Robots]. Marcombo Ediciones Tecnicas, Barcelona, Spain, ISBN: 9789701507582, Pages: 447 (In Spanish).
- Benhabib, B., A.A. Goldenberg and R.G. Fenton, 1985. A solution to the inverse kinematics of redundant manipulators. Proceedings of the IEEE Conference on American Control, June 19-21, 1985, IEEE, Boston, Massachusetts, USA., pp: 373-385.
- Campion, G., G. Bastin and B. D'Andrea-Novet, 1996. Structural properties and classification of kinematic and dynamic models of wheeled mobile robots. IEEE Trans. Robotics Automation, 2: 47-62.
- Craig, J.J., 1989. Introduction to Robotics Mechanics and Control. 2nd Edn., Addison-Wesley, Redwood City, CA., ISBN: 0201095289.
- Goldenberg, A., B. Benhabib and R. Fenton, 1985. A complete generalized solution to the inverse kinematics of robots. IEEE. J. Rob. Autom., 1: 14-20.
- Hernandez, M.O.D., 2014. [Teleoperation of a manipulator of 5 degrees of freedom using virtual platform]. Master Thesis, National Autonomous University of Mexico, Mexico City, Mexico. (In Spanish)
- Loukianov, A.A., Y.Q. Dai and M. Uchiyama, 1997. Trajectory tracking of spatial flexible link manipulators using inverse kinematics solution and vibration suppression. Proceedings of the 8th IEEE International Conference on Advanced Robotics ICAR97, July 7-9, 1997, IEEE, Monterey, California, ISBN:0-7803-4160-0, pp: 221-226.
- Mason, T.M., 2001. Mechanics of Robotics Manipulation. MIT Press, Cambridge, Massachusetts, ISBN:9780262133968, Pages: 253.
- Nino, J.J.Y., 2013. [Automatic control of a robot arm 5 degrees of freedom with arduino]. MSc Thesis, University of Valladolid, Valladolid, Spain. (In Spanish)
- Qu, B. and B. Xu, 2011. A control algorithm of general 6R mechanic arm based on inverse kinematics. Proceedings of the IEEE International Conference on Computer Science and Automation Engineering, June 10-12, 2011, IEEE, Shanghai, China, ISBN:978-1-4244-8727-1, pp: 327-330.
- Romero, A.A., 2012. [Design, print, mount and control a robotic manipulator]. Master Thesis, Charles III University of Madrid, Getafe, Spain. (In Spanish)
- Saquimux, C.R.B., 2005. [Design and construction of a robotic arm]. MSc Thesis, Universidad de San Carlos de Guatemala, Guatemala City, Guatemala. (In Spanish)
- Takahashi, T. and A. Kawamura, 2000. The high-speed numerical calculation method for the on-line inverse kinematics of redundant degree of freedom manipulators. Proceedings of the 6th IEEE International Workshop on Advanced Motion Control, March 30-April 1, 2000, IEEE, Nagoya, Japan, ISBN:0-7803-5976-3, pp: 618-623.